

June 23, 1992

RAPIDITY DISTRIBUTIONS OF  $K_s$  AND  $\Lambda$ 's PRODUCED BY  
14.6 GeV/c Si BEAMS ON Si and Pb TARGETS\*

Presented by S.J. Lindenbaum  
for the E-810 Collaboration

SEP 08 1992

A. Etkin, S.E. Eiserman, K.J. Foley, R.W. Hackenburg, R.S. Longacre,  
W.A. Love, T.W. Morris, E.D. Platner, A.C. Saulys  
*Brookhaven National Laboratory*

S.J. Lindenbaum  
*Brookhaven National Laboratory and City College of New York*

T.J. Hallman  
University of California, Los Angeles

C.S. Chan, E. Efstathiadis, M.A. Kramer, K. Zhao, Y. Zhu  
*City College of New York*

L. Madansky  
*Johns Hopkins University*

S. Ahmad, B.E. Bonner, J.A. Buchanan, C.N. Chiou,  
J.M. Clement, and G.S. Mutchler  
*Rice University*

Submitted to the 26th International Conference on High Energy Physics (ICHEP 92),  
August 6-12, 1992, Dallas, TX

MASTER

\* This research was supported by the US Department of Energy under Contract Nos. DE-AC02-76CH00016, DE-FG02-92ER40698, DE-FG02-91ER40645, DE-FG02-88ER40413 and DE-FG05-87ER40309, and the City University of New York PSC-BHE Research Award Program.

RAPIDITY DISTRIBUTIONS OF  $K_s$  AND  $\Lambda$ 's PRODUCED BY  
14.6 GeV/c Si BEAMS ON Si and Pb TARGETS\*

Presented by S.J. Lindenbaum  
for the E-810 Collaboration

A. Etkin, S.E. Eisenman, K.J. Foley, R.W. Hackenburg, R.S. Longacre,  
W.A. Love, T.W. Morris, E.D. Platner, A.C. Saulys  
*Brookhaven National Laboratory*

S.J. Lindenbaum  
*Brookhaven National Laboratory and City College of New York*

T.J. Hallman  
University of California, Los Angeles

C.S. Chan, E. Efstathiadis, M.A. Kramer, K. Zhao, Y. Zhu  
*City College of New York*

L. Madansky  
*Johns Hopkins University*

S. Ahmad, B.E. Bonner, J.A. Buchanan, C.N. Chiou,  
J.M. Clement, and G.S. Mutchler  
*Rice University*

## ABSTRACT

Excess strangeness production is an expected signal for formation of a Quark-Gluon Plasma and therefore we have been searching for it. We present the first measurements at AGS energies of rapidity distributions of  $K_s$  and  $\Lambda$  production with Silicon beams on Silicon and Lead targets. The measurements cover the lab rapidity region of  $2.0 < y < 3.5$  for  $K_s$  and  $1.4 < y < 3.2$  for  $\Lambda$ 's. The gross features of our observation are explainable with a nuclear cascade model including  $N^*$  (isobaric nucleon) as a significant source of strangeness. The various models used to compare with the data are discussed in the paper.

### 1. Introduction

We have previously presented results of  $K_s$  and  $\Lambda$  production from Cu and Au targets [1]. Here we report on 817  $K_s$  and 1122  $\Lambda$ 's from Si target and 1445  $K_s$  and 2147  $\Lambda$ 's from Pb target, "centrally" produced.

---

\* This research was supported by the US Department of Energy under Contract Nos. DE-AC02-76CH00016, DE-FG02-92ER40698, DE-FG02-91ER40645, DE-FG02-88ER40413 and DE-FG05-87ER40309, and the City University of New York PSC-BHE Research Award Program.

## 2. Experimental Method

The experimental method was described in a previous publication [1]. This experiment measured charged tracks in the forward hemisphere in the center-of-mass in three TPC (Time Projection Chamber) modules with a 5 kG magnetic field. The trigger, as described in Ref. 1 selected centrally enriched events for data recording. The final centrality selection of the data sample presented here is described below. Target thicknesses were selected to minimize gamma ray conversion which would give incorrect hadron multiplicities. We used a 0.122 cm thick Si target (1.3% radiation length) and a 0.02 cm thick Pb target (3.5% radiation length).

## 3. Data Analysis

Events were reconstructed, with multiplicities of charged tracks ranging up to 100, using a three-dimensional tracking program. The reconstructed interaction point was required to be in the target. This data set consists of 91,393 interactions in the Si target and 109,838 interactions in the Pb target. For the final data sample we selected the most central events using the multiplicity of the negatively charged tracks within our good acceptance as a centrality selector. *Since there is no way of measuring the exact impact parameter of the interaction, we found this to be a reasonably good measure of the centrality from both the increased yield of  $K_s$  and  $\Lambda$  production [1] as a function of this multiplicity and from Monte Carlo studies of the correlation of impact parameter with this multiplicity we also concluded it is a reasonable measure of centrality.* We selected central events from the Si target by requiring this negative multiplicity to be  $> 11$ , corresponding to a cross section of approximately 120 mb, and for Pb we required this multiplicity to be  $> 13$ , corresponding to a cross section of approximately 280 mb. These cross sections are generally similar to what other experiments have used (e.g. E-802). This selection criterion resulted in 12,679 central events from the Si target and 15,438 events from the Pb target.

Tracks which missed the interaction point by more than 7 mm were selected as candidates for decay vertices. To reduce combinatorial background for decay vertices, we required the decay point to be more than 10 cm downstream of the interaction point and the reconstructed momentum vector was required to point back to the production vertex within 2.5 mm. In addition, in order to select tracks which had good momentum resolution, we required the sagitta of the measured tracks to be  $> 0.375$  cm. Since we have no particle identification in our experiment, the effective masses for  $K_s$  and  $\Lambda$ 's were calculated by kinematic hypothesis only by assigning a proton or a pion mass to the charged tracks. Figure 1 shows the result of the effective mass calculation for  $\pi^-\pi^+$  hypothesis and Fig. 2 shows the result of the proton  $\pi^-$  hypothesis for our final selected data sample from the Pb target. Decay vertices with effective masses in the range of 0.475-0.525  $\text{GeV}/c^2$  were selected as  $\Lambda$ 's. As can be seen, the  $K_s$  and  $\Lambda$  signals are quite large compared to the  $< 10\%$  backgrounds. In all cases the tails of the effective mass distributions were used for background subtractions. Since there is considerable kinematic overlap between  $K_s$  and  $\Lambda$ 's, Fig. 1 has decay vertices removed if they satisfy the  $\Lambda$  hypothesis. Because of phase space considerations, there is no significant background for  $\Lambda$ 's due to  $K_s$ , therefore no  $K_s$  candidates were removed for Fig. 2 (or the final data sample).

The acceptance corrections of the rapidity distributions which we present in this paper were performed with a complete Monte Carlo simulation of the effects of the apparatus and cuts to our final data sample. Events were generated using an AGS HIJET model [2]. The GEANT3 program was used to track the generated tracks through a magnetic field and the resultant signals in the TPC were written out in the same format as our recorded data. The generated hits included all the known effects of detector apertures, efficiencies and distortions. The results of this simulation were then analyzed by the same program used to analyze the actual data, including the tracking. 300,000 interactions in each target were generated and analyzed. The reconstructed rapidities ( $y$ ) and transverse momenta<sup>2</sup> ( $pt^2$ ) for  $K_s$  and  $\Lambda$ 's were binned in a  $6 \times 7$  matrix in  $y$  and  $pt^2$  for both the generated and surviving events in the rapidity range of  $1.4 < y < 3.2$  for  $\Lambda$ 's and  $1.7 < y < 3.5$  for  $K_s$ , and transverse momentum<sup>2</sup> range of  $0 < pt^2 < 1.0$  for both. The ratio of these matrices represented our acceptance and were used to correct the analyzed data in a  $6 \times 7$  acceptance grid. The  $K_s$  acceptance was in the range of 5 - 20% and the  $\Lambda$  acceptance was in the range of 3 - 12% including the correction for neutral decays.  $K_s$  data in the rapidity range of  $1.7 < y < 2.0$  was not used because of a rapid variation of acceptance as a function of  $pt^2$ .

#### 4. Results

In Figs. 3 and 4 we have plotted the rapidity distributions of  $K_s$  from the Si and Pb targets, respectively. In Figs. 5 and 6 we have plotted the same distributions for  $\Lambda$ 's. The curves shown in the figures are the predictions of several models. Also shown on Figs. 3 and 5 are the measured rapidity distributions for  $p + p \rightarrow K_s$  or  $\Lambda + X$  at 12 GeV/c [ref] scaled up by a factor of 28 to account for the 28 nucleons in the Si nucleus. The rapidity distributions for Si were measured only for forward rapidities, but reflected about  $y = 1.7$  because of the symmetry of the reaction. In this way we obtain a measurement of the whole rapidity distribution.

In Fig. 4 we have plotted  $[dN/dy(K^+) + dN/dy(K^-)]/2$  for Si + Au interactions, the only other published rapidity measurements of strange particle production from nuclei at our energy [4]. We expect, from the quark model, that this average  $K^+, K^-$  cross section should be the same as  $dN/dy(K_s)$ . Considering that the measurements were on a lighter target and are at a different rapidity, we observe good agreement with the results of Ref. 4.

Our data are consistent with an exponential dependence in transverse mass ( $m_t = \sqrt{m_0^2 + pt^2}$ ). We do not have adequate statistics in this data sample to determine the inverse slope of the exponential as a function of rapidity. In order to find the total cross section in each rapidity bin we have performed fits in  $y$  and  $m_t$  space to the four sets of data shown, using two hypotheses: 1) the inverse slope is a constant independent of  $y$ , and 2) we introduced a term in the fit where the inverse slope has a  $\cosh(y)$  dependence added. In each case we obtained a better or equal  $\chi^2$  possibility with the  $\cosh(y)$  term, but statistics do not allow us to rule out an inverse slope independent of rapidity. The "exponential temperatures" range from 160-240 MeV with higher temperatures favored for the  $\Lambda$ 's. The figures show the integrals using the  $\cosh(y)$  term in the fit. The errors were obtained by mapping a  $\chi^2$  contour of  $1\sigma$  away from the best fit, since the integration of

an exponential involves folding errors of two correlated variables - the intercept and slope of the exponential.

### 5. Discussion and Conclusions

The first thing to be noted is that our Si data cannot be described by a pure superposition of 28 nucleons with the other 28 nucleons in the two silicon nuclei. This has been previously observed at higher energies in S + S reactions [5]. Nuclear rescattering needs to be invoked in order to try to explain the excess cross section for  $K_s$  and  $\Lambda$  production.

The dotted line in Figs. 3-6 represents AGS HIJET [2b] predictions for each case. AGS HIJET[2b] is a modification of Ref. 2a in order to better simulate the physics. HIJET underpredicts the  $K_s$  yield by a factor of two. Each successive collision of the initial nucleons in the HIJET simulation is based on nucleon-nucleon data. When nucleons interact at these energies they become excited into  $N^*$  which on the average decay into  $\Lambda K$  about 2.5% of the time. For a central Si-Si collision one would expect that nearly all the 56 nucleons would be excited into  $N^*$ 's, thus leading to around 1.5  $\Lambda$ 's per event. At the AGS energies the main sources of strange particles are  $N^*$  decay or associated production, while K pairs are a minor source whose production sharply depends on the collision energy. AGS HIJET was therefore modified by making  $N^*$  a propagation mode in the system. When an  $N^*$  is formed, it was allowed to propagate to the next collision. This procedure did not increase the number of  $N^*$ 's but did create higher energy collisions thus increasing the number of K pairs produced. The results of this addition are shown on Figs. 3-6 as a dashed line. It can be seen that this addition improves the  $K_s$  yield to the point that it is not in bad agreement with the data.

The solid curves on Figs. 3-6 represent the predictions of the ARC (A Relativistic Cascade) model [6]. The calculations for the curves were obtained as a private communication from the authors of the model. As can be seen the ARC model represents the  $\Lambda$  rapidity data well. It seems to have the wrong functional form as a function of rapidity for  $K_s$ , underpredicting at mid rapidity and overpredicting at high rapidity, although the total number of  $K_s$  looks about right.

In conclusion we find that our measured rapidity distributions of  $K_s$  and  $\Lambda$ 's produced by Si beams on Si and Pb targets cannot be accounted by superposition of nucleon-nucleon interactions, but a nuclear cascade model of the reaction including  $N^*$  production must be used to account for most of the strangeness.

## References

1. S.E. Eiseman *et al.*, Phys. Lett. B248 (1990) 254.
- 2a. A. Shor and R. Longacre, Phys. Lett. B218 (1989) 100. We made further modifications to better simulate the physics for the AGS HIJET version we used.
- 2b. AGS HIJET. E-810 version of Ref. 2a to which further modifications were made to better simulate the physics.
3. V. Blobel *et al.*, Nucl. Phys. B69 (1974) 454.
4. T. Abbott *et al.*, Phys. Rev. Lett. 66 (1991) 1567.
5. A. Bamberger *et al.*, Z. Phys. C43 (1989) 25.
6. Y. Pang, T.J. Schlagel, and S.H. Kahana, Phys. Rev. Lett. 68 (1992) 2743.

## Figure Captions

Fig. 1 Effective mass plot of the  $\pi^+\pi^-$  hypothesis for decay vertices from Pb target with vertices removed if they satisfy the  $\Lambda$  effective mass cuts.

Fig. 2 Effective mass plot of the proton  $\pi^-$  hypothesis for decay vertices from Pb target.

Fig. 3 Rapidity distribution for  $K_s$  from the Si target. The solid points above a rapidity of 1.7 are our measurements. Errors shown are statistical only. The solid points below rapidity of 1.7 are our measurements reflected about 1.7. The open circles represent the measurements of Ref. 3 scaled up by 28. The solid curve is the prediction of the ARC model. The dashed curve is the prediction of the AGS HIJET with  $N^*$ 's included in the model. The dotted curve is the prediction of the AGS HIJET.

Fig. 4 Rapidity distribution for  $K_s$  from the Pb target. The solid points are our measurements. Errors shown are statistical only. The open circles are the average values of  $K^+$  and  $K^-$  measurements of Ref. 4. The curves are the predictions of the various models as defined in Fig. 3 caption.

Fig. 5 Rapidity distribution for  $\Lambda$ 's from the Si target. The solid points above a rapidity of 1.7 are our measurements. Errors shown are statistical only. The solid points below rapidity of 1.7 are our measurements reflected about 1.7. The open circles represent the measurements of Ref. 3 scaled up by 28. The curves are the predictions of the various models as defined in Fig. 3 caption.

Fig. 6 Rapidity distribution for  $\Lambda$ 's from the Pb target. The solid points are our measurements. Errors shown are statistical only. The curves are the predictions of the various models as defined in Fig. 3 caption.

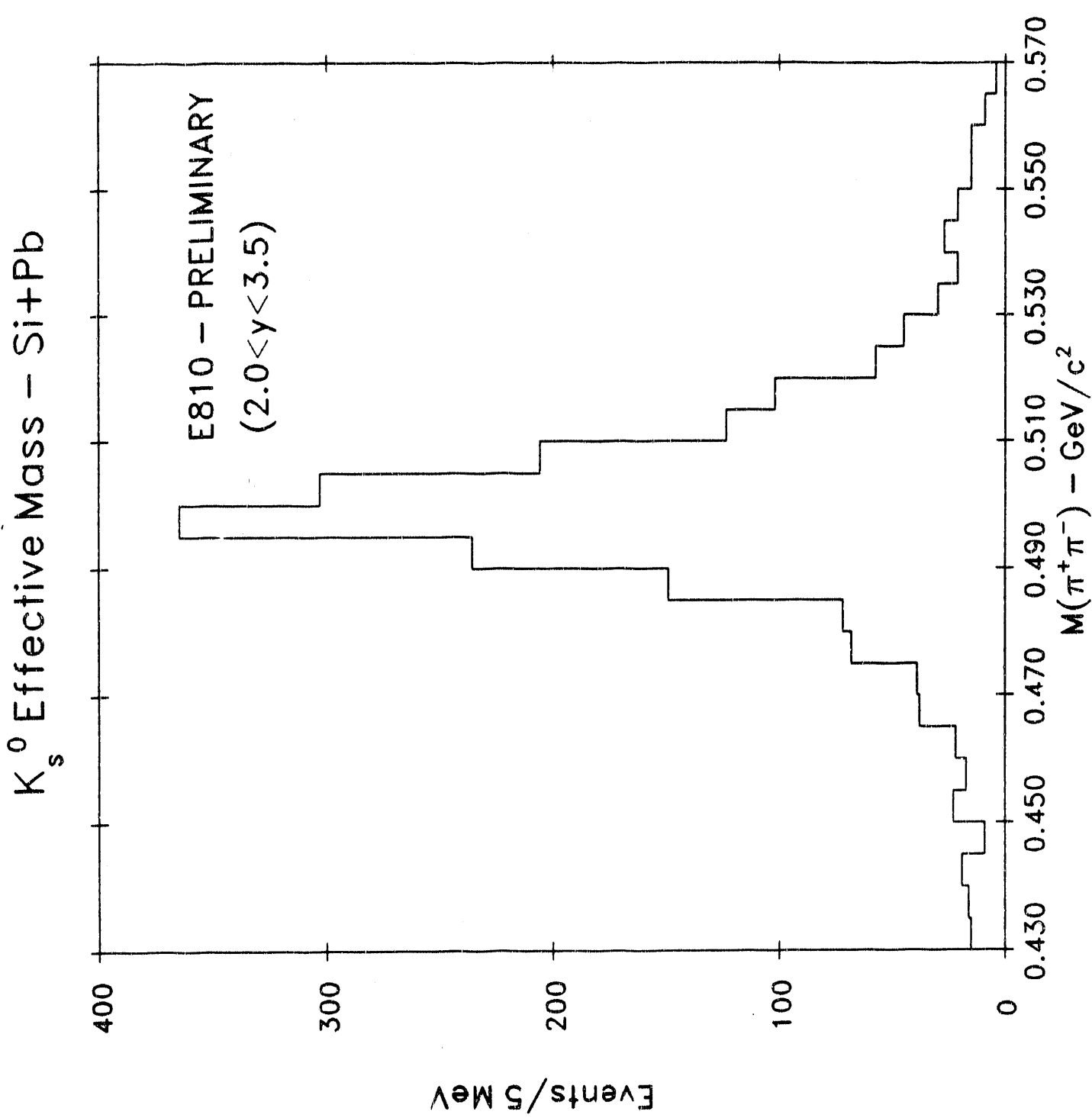
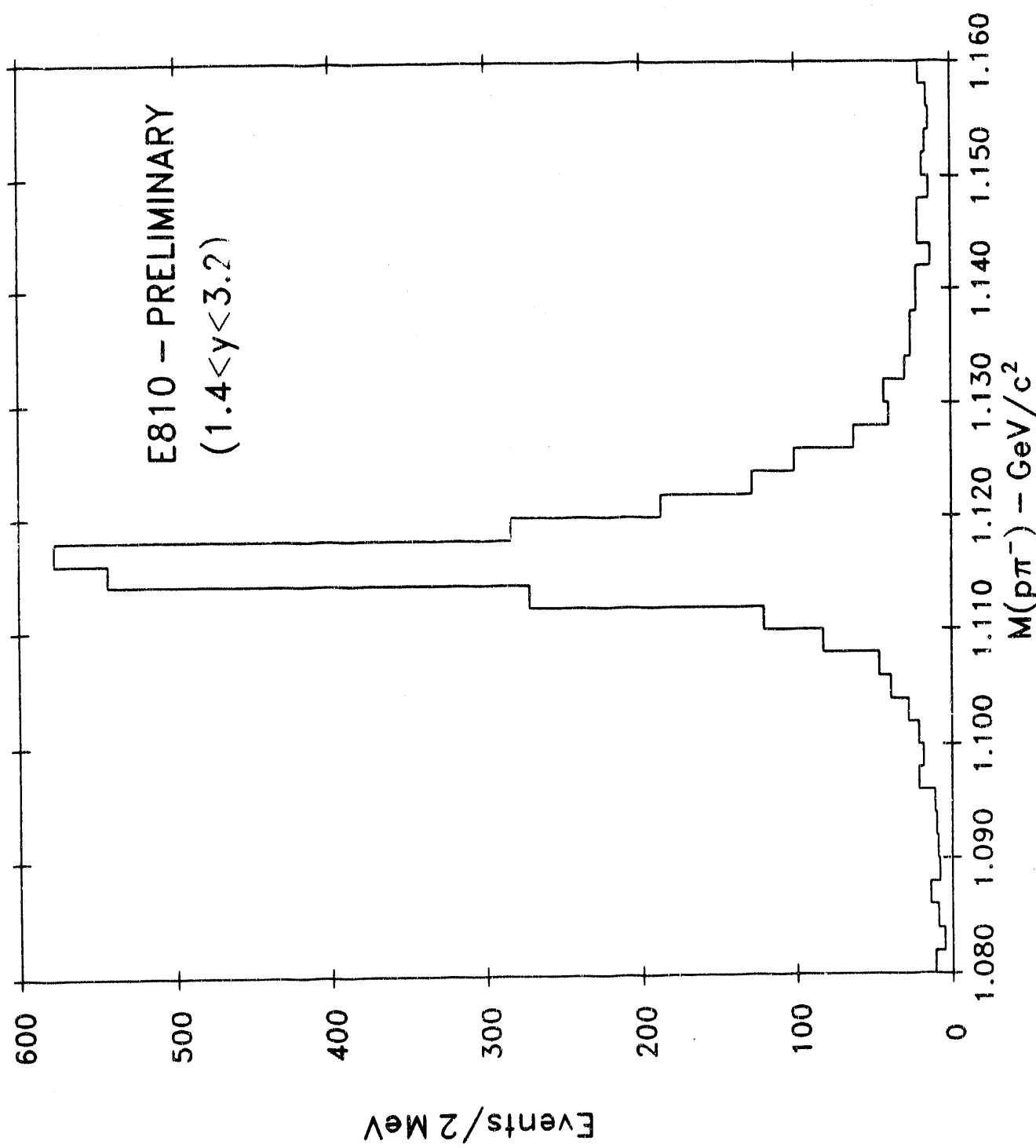


Figure 1

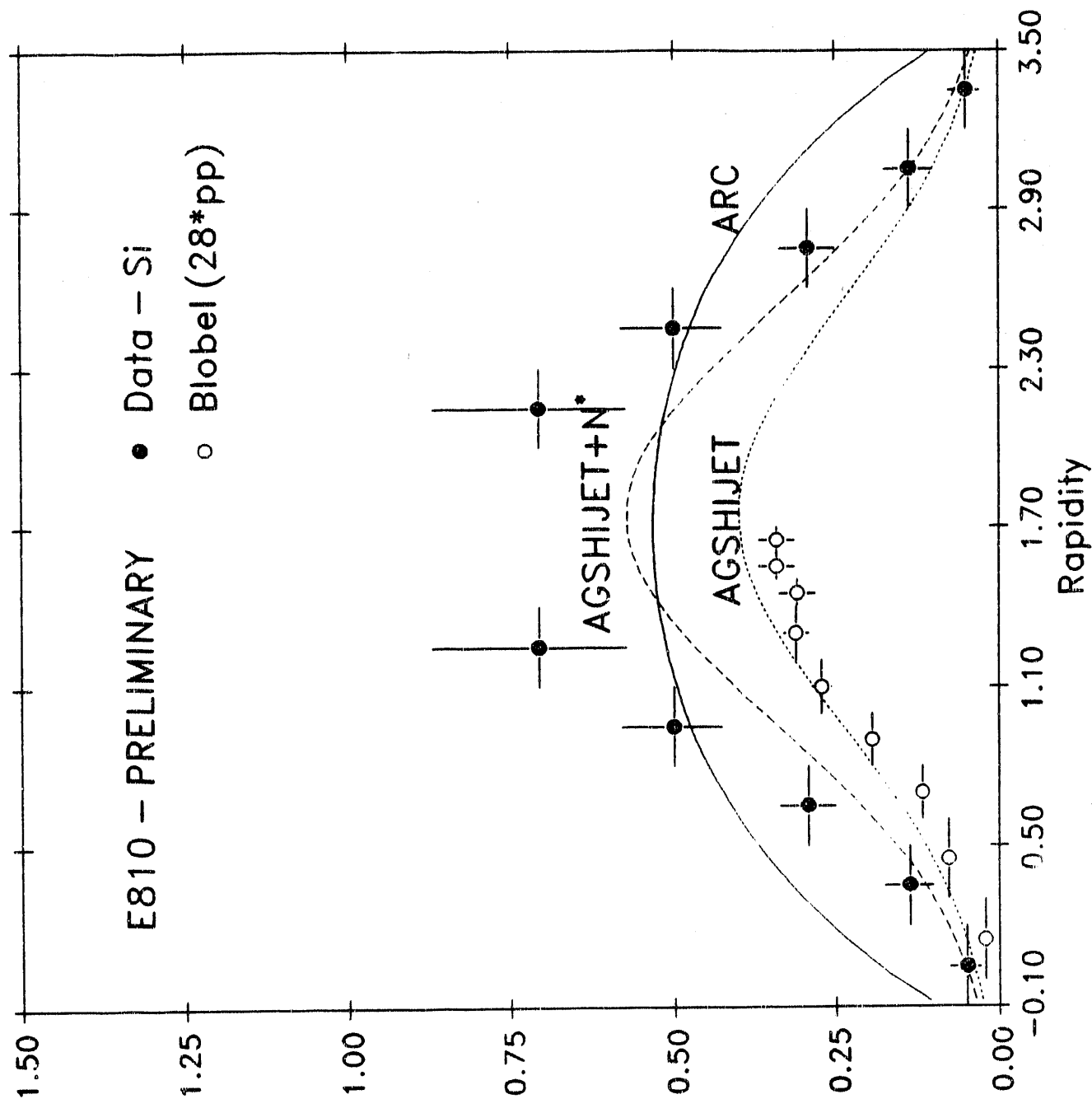
# $\Lambda$ Effective Mass — Si+Pb



Si on Si -  $K_s^0$  Rapidity

E810 - PRELIMINARY     ● Data - Si  
                                  ○ Blobel (28\*pp)

$\lambda p/Np^* N/1$



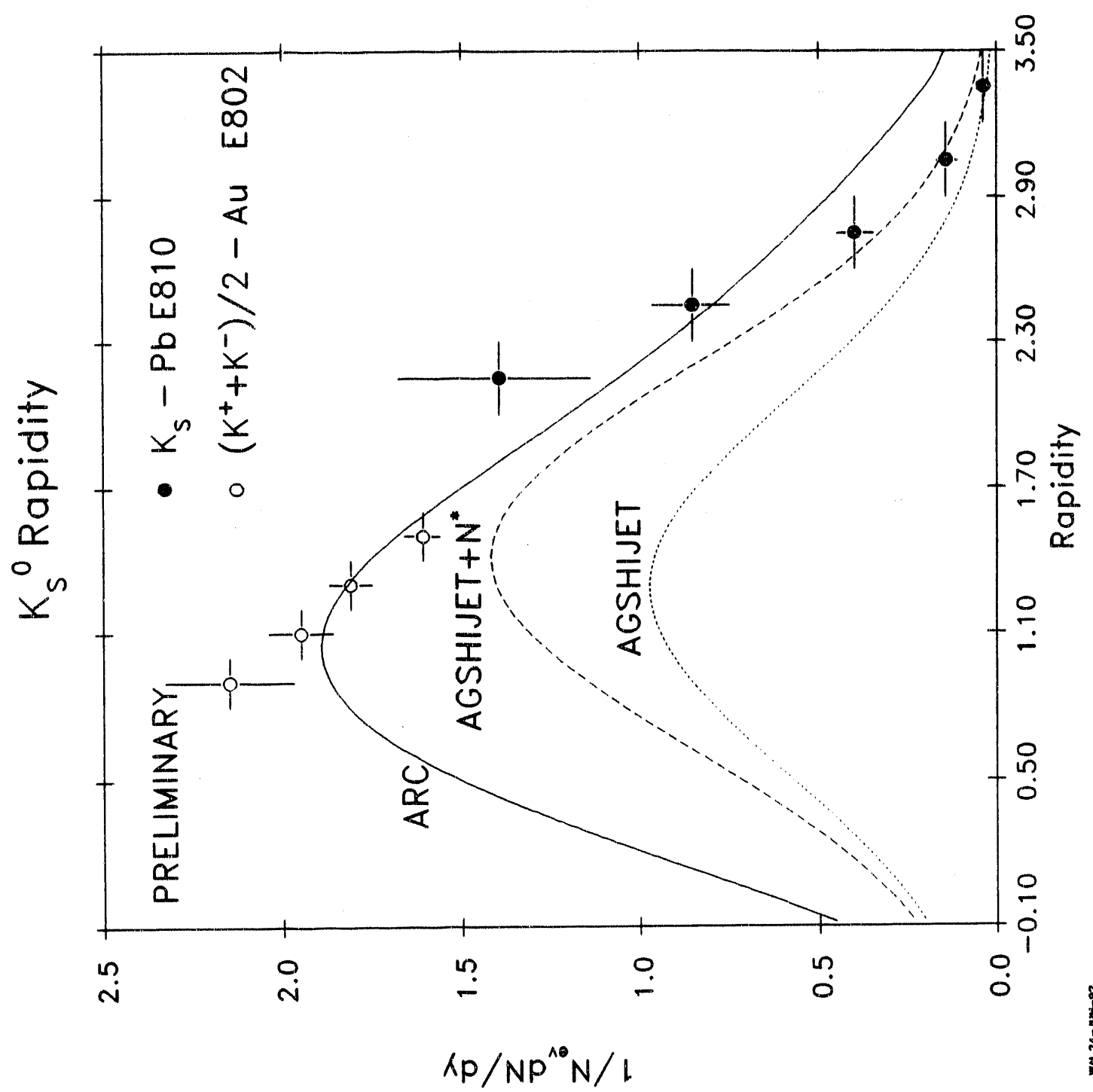


Figure 4

Si on Si -  $\Lambda$  Rapidity

E810 - PRELIMINARY     ● Data - Si  
(28\*pp Biobel)

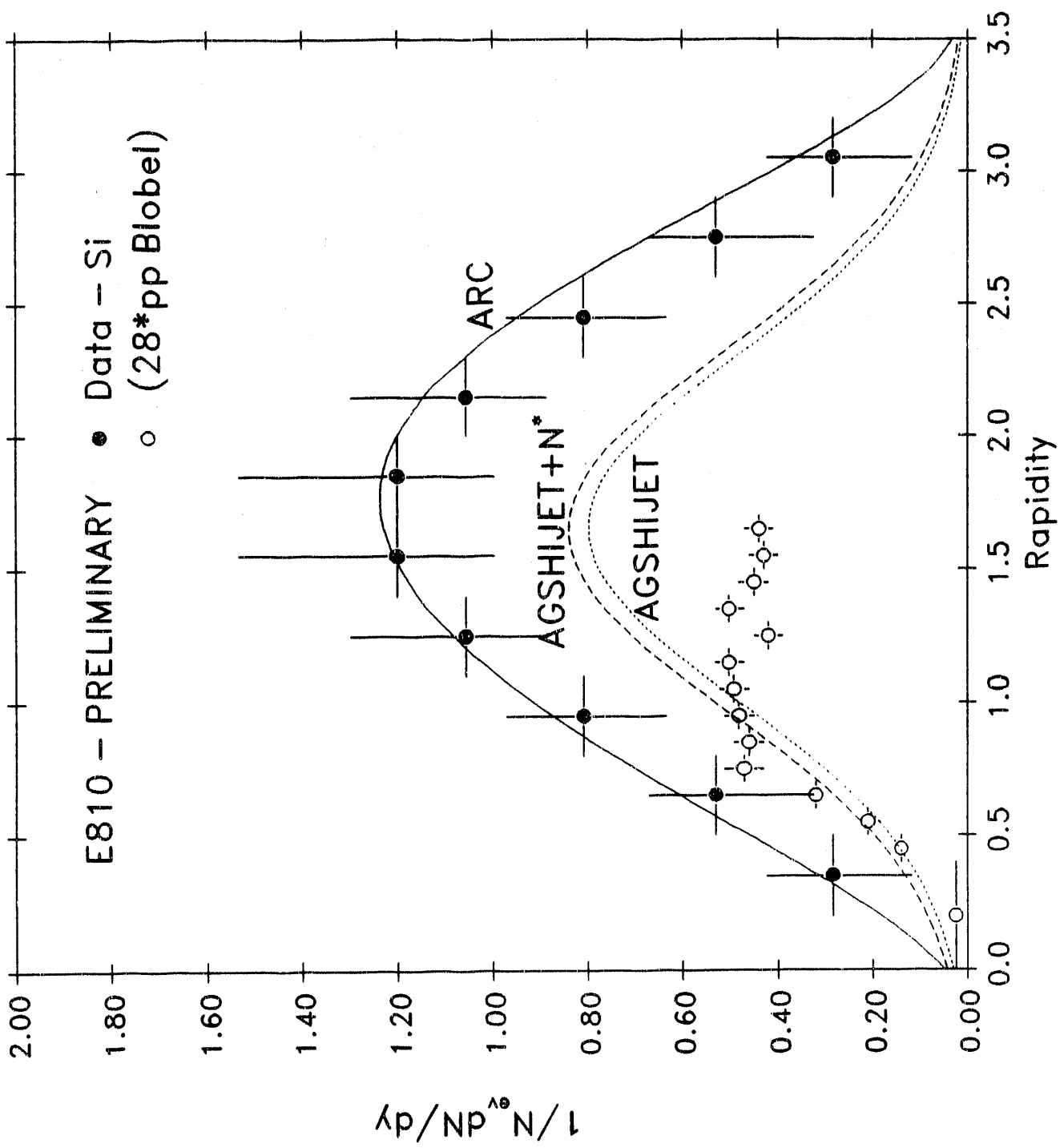
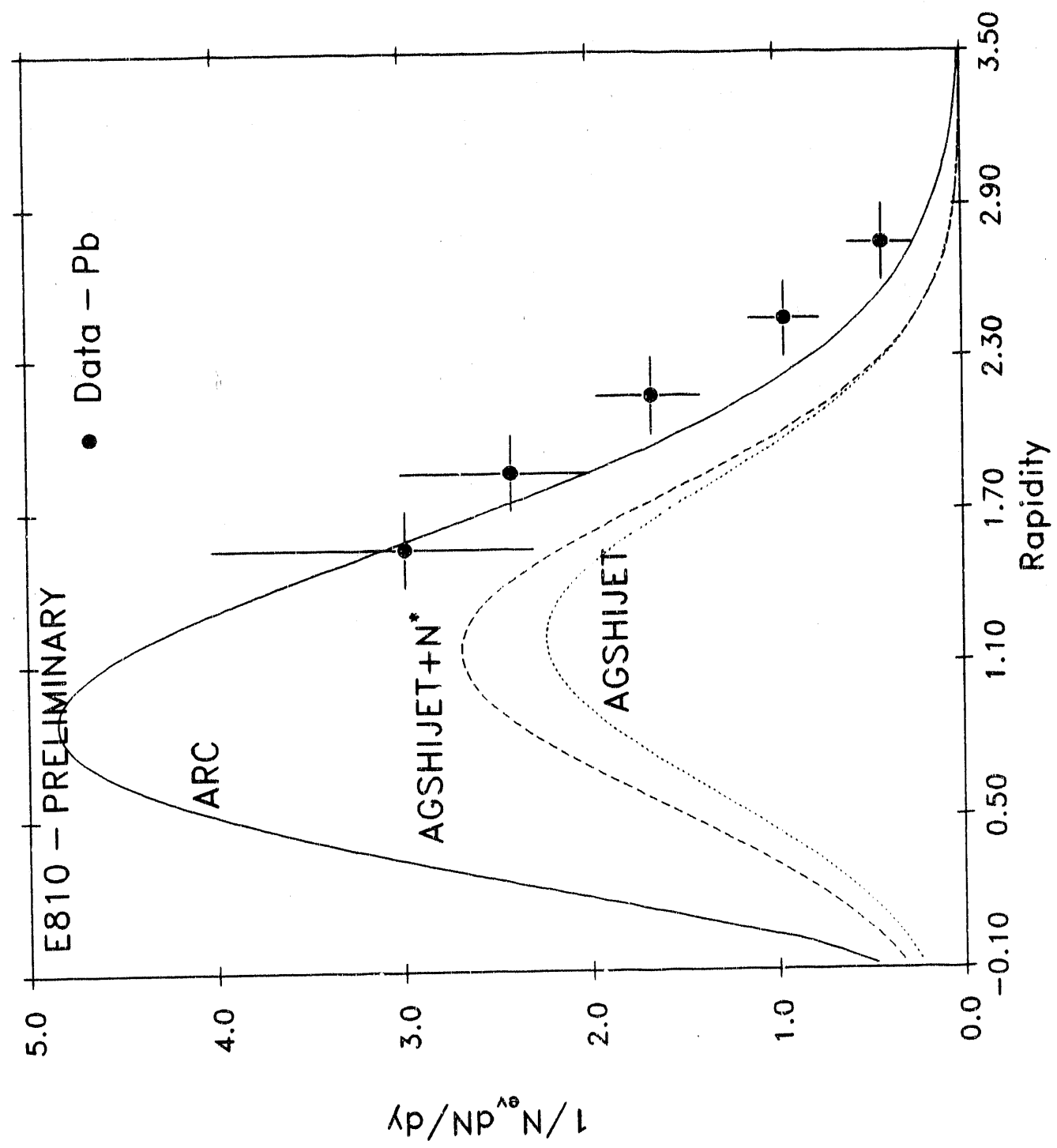


Figure 5

# Si on Pb - $\Lambda$ Rapidity



END

DATE  
FILMED

10/29/92

